The Journal of Experimental Biology 216, 1152-1159

doi:10.1242/jeb.078931

RESEARCH ARTICLE

Flow-dependent porosity and other biomechanical properties of mysticete baleen

Alexander J. Werth
Department of Biology, Hampden-Sydney College, Hampden-Sydney, VA 23943, USA
awerth@hsc.edu

SUMMARY

Despite its vital function in a highly dynamic environment, baleen is typically assumed to be a static material. Its biomechanical and material properties have not previously been explored. Thus I tested sections of baleen from bowhead whales, *Balaena mysticetus*, and humpback whales, *Megaptera novaeangliae*, alone or in groups representing miniature 'racks', in a flow tank through which water and buoyant particles circulated with variable flow velocity. Kinematic sequences were recorded through an endoscopic camera or viewing window. One set of experiments investigated particle capture; another series analyzed biomechanical behavior, including fringe spacing, movement and interaction. Baleen fringe porosity directly correlates, in a mostly linear fashion, with velocity of incident water flow. However, undulation and interaction of fringes (especially of bowheads) at higher flow velocities can decrease porosity. Fringe porosity depends on distance from the baleen plate. Porosity also varies, with fringe length, by position along the length of an individual plate. Plate orientation, which varied from 0 to 90 deg relative to water flow, is crucial in fringe spacing and particle capture. At all flow velocities, porosity is lowest with plates aligned parallel to water flow. Turbulence introduced when plates rotate perpendicular to flow (as in cross-flow filtration) increases fringe interaction, so that particles more easily strike fringes yet more readily dislodge. Baleen of bowhead whales, which feed by continuous ram filtration, differs biomechanically from that of humpbacks, which use intermittent lunge filtration. The longer, finer fringes of bowhead baleen readily form a mesh-like mat, especially at higher flow velocities, to trap tiny particles.

Key words: Cetacea, mysticete, whale, filter feeding, biomechanics, hydrodynamics.

Received 7 August 2012; Accepted 24 November 2012

INTRODUCTION

Baleen is not a static material. The filtering apparatus of whales (Cetacea: Mysticeti) is usually compared to a net or sieve, but unlike nets and sieves baleen is a variable filter whose pore size is not set during construction but rather determined during use. Baleen withholds trapped prey as water streams through or across its plates (laminae) and hair-like tubular fringes, also referred to as baleen bristles, filaments, fibers or hairs (Williamson, 1973). Despite baleen's long-understood vital function in this highly dynamic environment, the biomechanical and material properties of this substance have not previously been explored. In fact, baleen's direct role in feeding has not been sufficiently addressed. The past decade has witnessed extraordinary advances in our understanding of mysticete feeding, chiefly with data from digital tags deployed on foraging whales (Goldbogen et al., 2006; Goldbogen et al., 2007; Goldbogen et al., 2008; Friedlaender et al., 2009; Simon et al., 2009; Goldbogen et al., 2011; Nowacek et al., 2011; Ware et al., 2011; Goldbogen et al., 2012), often combined with computational modeling of lunge feeding (Potvin et al., 2009; Potvin et al., 2010). Although these results offer detailed information (from hydrophones, depth recorders, accelerometers and video) on precise links between mysticete locomotion and prey engulfment, they do not offer information on the dynamic forces and flows within the mouth of mysticetes, particularly as it involves the baleen filter.

Mysticete filter feeding is either intermittent or continuous (Werth, 2000). Intermittent filter feeders engulf and remove food particles (aggregated prey) from a discrete mouthful of water. Whales that use this feeding mechanism (blue, fin, humpback and other rorqual or 'groove-throated' whales of the Family Balaenopteridae, as well as the gray whale, Eschrichtiidae) possess special anatomical adaptations for intermittent feeding (Pivorunas 1977; Pivorunas, 1979; Lambertsen, 1983; Pyenson et al., 2012). Just as the loose mandibular joint, intermuscular fascial throat pouch, accordion-like gular pleats and flaccid, deformable tongue of rorquals reflect their lunge feeding, balaenid (bowhead and right whale) oral morphology is suited for continuous filtration of tiny (~1 mm) prey. The subrostral gap, a cleft between baleen racks below the tip of the rostrum, and orolabial sulcus, a gutter-like depression medial to the lip – specific features of the balaenid oral cavity that promote continuous, unidirectional water flow – are singular among mysticetes, as are the exceptionally long (up to 4 m), springy, finely fringed baleen, fused cervical vertebrae, firm tongue and high semicircular lips extending above the mandibles to enfold the narrow, arched rostrum (Werth, 2000). In balaenids, baleen both captures and retains prey, whereas in intermittent filter-feeding mysticetes, baleen retains prey caught by the expanded oral cavity during feeding events (Pivorunas, 1979; Werth, 2000). Balaenids 'clean' their baleen of accumulated prey at varying intervals depending on prey density (Werth, 2001).

Little has been published regarding baleen function. There have been studies of baleen's microscopic ultrastructure (Pfeiffer, 1992), calcification (Szewciw et al., 2010), and histology and development (Tullberg, 1883; Pivorunas, 1976; Fudge et al., 2009), along with mentions of its general properties (St Aubin et al., 1984; Orton and Brodie, 1987; Lambertsen et al., 2005). Aside from two publications on baleen's filtration capacity and trophic efficiency based on flume

testing (Mayo et al., 2001; Werth, 2012), studies of baleen function include unpublished reports (Braithwaite, 1983; Lambertsen et al., 1989) and master's or doctoral theses (Kot, 2005; Kot, 2009; Pinto, 2011; Young, 2012). No prior publications describe, let alone acknowledge, the crucial dynamic nature of the baleen filter or investigate its active characteristics. This paper presents the first data demonstrating that baleen is a dynamic material whose biomechanical characteristics are dependent on the velocity and direction of flow.

Specifically, this comparative functional study explored porosity (ϕ) and related properties of baleen samples from balaenid (bowhead, *Balaena mysticetus* Linnaeus 1758) and balaenopterid (humpback, *Megaptera novaeangliae* Borowski 1781) whales in a circulating flow tank, testing different flow regimes and baleen orientations. The objective was to measure how these different baleen types capture particles under varying flow patterns, and to determine, *via* kinematic study of videotaped sequences, how fringes of individual and multiple plates move and interact to effect such capture. A basic morphometric analysis of fringe measurements and density was first conducted to determine how species-specific baleen differences relate to the biomechanical 'behavior' of fringes and thus to ϕ and particle/prey capture.

MATERIALS AND METHODS

Experimental specimens

Samples of baleen from multiple plates were used for morphometric analysis and flow tank testing. These were full or main plates (Williamson, 1973), from the basal layer at the gum line to terminal fringes. Baleen samples were kept submerged in flowing water for at least 7 days prior to flow tank testing. All bowhead baleen specimens were obtained from adult whales hunted by Inupiat Eskimos of Barrow, Alaska. Tissues were collected under permit no. 519 issued by the National Marine Fisheries Service (NMFS) to T. F. Albert of the North Slope Borough, AK, Department of Wildlife Management. Plates of humpback baleen were obtained from stranded animals by the Edgerton Research Laboratory of the New England Aquarium, Boston, MA, under NMFS permit no. 932-1489. Nothing is known of the animals from which the baleen specimens were taken (sex, age, body length, etc.). Although plate length and curvature reveal the general position within the baleen rack from which plates were taken, no other morphological differences whatsoever were observed in baleen specimens of a particular species. Whole plate dimensions were not recorded because some were damaged, but never on the fringed, lingual edge; this did not affect the smaller sections used for experimental testing, all of which were undamaged and of the same size (20×7 cm, excluding fringes).

Baleen morphometry

The number of fringes at any location along a baleen plate margin depends on the angle at which the hair-like fringes emerge from the plate's keratinous, calcified cortical matrix that encloses the central tubular region in a sandwich-like array (Pivorunas, 1976) (Fig. 1). Because this determines comparative porosity, ϕ, fringes of six plates each of bowhead and humpback baleen were counted (Table 1). Differences were recorded at four locations along each triangular plate: just below the broad, dorsal base of the plate where it emerges from the palate; just above the narrowest, ventral-most terminal vertex; and at two equidistant sites between these extremes, at one- and two-thirds the length of the plate (Fig. 1). Fringes were counted at each site (a point location) if they originated there or originated dorsally and hung free at the site. In addition, fringes were counted along a 1 cm length (centered on the four points) to yield density in fringes cm^{-1}. Dimensions of fringe length and diameter were also measured (Table 1).

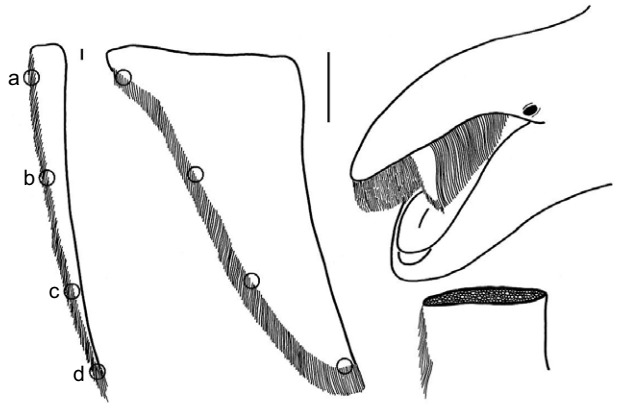

Fig. 1. Schematic diagram showing morphometry of triangular baleen plates of bowhead (left) and humpback whales, showing four locations of measurement of mean density of fringes freely emergent from overlying keratinous matrix (a, most dorsal/proximal, at base; d, most ventral/distal, at vertex). Only free fringes were counted (dry). Scale bars, 10 cm. Also shown in diagrammatic representation are a generic whale mouth with full and partial baleen racks [showing position of a single plate, at front of the partial rack, with other plates (laminae) arrayed posterior to it], and a schematic cross-section of a plate's distal portion showing central horn tubules sandwiched between layers of cortical matrix. When exposed by abrasion, the central tubules emerge on the lingual (medial) margin as fringes.

Flow tank testing

Cut baleen sections (each 20 cm long × 7 cm wide) were secured by clamping to a metal rod, individually or in groups of six laminae, to create a miniature 'rack' of baleen, and submerged below the water surface in a 901 circulating flow tank (flume). Multiple plates were spaced 1 cm apart, as *in vivo*. The tank was made of PVC in a vertical loop, modeled on a design by Vogel (Vogel, 1996), with a transparent Plexiglas top in which a completely flat viewing window was installed and through which a ruled grid behind the test chamber could be seen. The working section of the tank's test chamber had a length of 70 cm and a cross-sectional area of 900 cm^2, with 1–2% blockage due to the tissue samples. The rod holding the baleen specimens was secured to the top rim of the testing chamber. Flow through the tank was modulated three ways: selecting five motor speeds, using impellers of different diameter, and adjusting a rheostat to alter input voltage to the motor. Flow velocity, v, varied from 5 to 140 cm s^{-1} in experiments. Before and after experimental trials, v was calibrated with a digital flow meter (model MFP51, Geopacks, Hatherleigh, Devon, UK). Most trials were performed with v ranging from 10 to 120 cm s^{-1}, which accords with published swimming speeds of bowhead whales skimming at the surface or deeper in the water column (Reeves and Leatherwood, 1985; Carroll et al., 1987; Lowry, 1993; Nowacek et al., 2001), and is at or just below the locomotor speeds of humpback whales at the end of lunge-feeding events (Goldbogen et al., 2008), when filtration is presumed to occur. Simon et al. (Simon et al., 2009) reported an average locomotor speed for feeding bowheads of 75 cm s^{-1}, which would be the same v for flow past bowhead baleen given the continuous ram filtration of this species. Goldbogen et al. (Goldbogen et al., 2007) estimated the flow past baleen of lunge-feeding fin whales at 80 cm s^{-1}, which should be nearly the same in humpback whales, as indicated by research of scaling effects in rorquals (Goldbogen et al., 2012).

Table 1. Baleen fringe counts, density, length and diameter for humpback and bowhead whales

Species	Count, density (cm^{-1})					Fringe length (mm)	Fringe diameter (mm)
	Site a	Site b	Site c	Site d	Overall		
Humpback	8±1.3, 12±3.4	9±1.4, 24±3.9	11±1.7, 28±4.0	26±2.5, 43±7.1	13.5±2.1, 35.6±5.4	92±17.8	0.66±0.04
Bowhead	17±2.2, 31±4.6	21±2.6, 47±4.9	32±3.7, 84±6.2	39±5.8, 158±9.7	27.3±3.9, 106.7±7.4	194±12.5	0.23±0.02

Data (means ± s.d.) are averaged from six plates of each species. Number of fringes freely separated from the overlying matrix were counted at individual points (sites a–d; Fig. 1) and over a 1 cm segment of plate margin centered on each count site to yield density in fringes cm^{-1}. Length and diameter values are averaged from all four sites (a–d).

Initial tests were performed in fresh tap water at 19°C; later tests were performed in freshwater or seawater at temperatures ranging from 13 to 24°C. Plates were submerged in water before flow commenced. Individual baleen plates and 'mini-racks' were placed in varying positions, initially with the medial (lingual) fringe-bearing side of the plate facing 'upstream', representing flow of water from the inside to the outside of the mouth, as occurs during mysticete filtration. Later tests involved rotating the fixed single or multiple plates from this initial position (i.e. 0 deg relative to the incident water flow), for a different angle of attack, α, all the way to 90 deg (perpendicular to water flow) or in intermediate positions of 30 or 60 deg to water flow (Fig. 2). All trials were conducted five times for each set of variables, with ANOVA testing of data from replicates.

One experimental series investigated particle capture by baleen plates and fringes. After experimenting with several types of particles, including brine shrimp (*Artemia*) eggs, air bubbles, and reflective or opaque glass and polymer microspheres, the final trials (described here) utilized solid, non-sticking latex polymer beads (Sargent-Welch 50024, Buffalo, NY, USA). The beads are bright blue, neutrally buoyant (1 g cm^{-3}) and have a mean particle size (diameter) of 710 μm. Density was not varied in these experiments but held constant at approximately 15,000 particles m^{-3}. Flow meter records of v were verified by video analysis of free particle movement relative to the ruled (1×1 cm) background. In many instances suspended particles made incidental contact with, but did not remain trapped on, baleen fringes; such particles were carried away by water flow or, in some cases, were swept away by undulation of other fringes. For the purposes of this study, particles were deemed captured if they remained in contact with baleen for at least two consecutive seconds based on the kinematic analysis of videotaped sequences described below. Particle capture rates displayed in figures are calculated according to trapping of new particles per second (not per 2 s). Capture was defined with a minimum 2 s interval partly for logistical reasons, because many particles were observed to make momentary (~1 s) contact with baleen, and to bounce or slide (Sanderson et al., 2001) along the filtering fringes. This higher standard for capture (>1 s) also better represents real-world filtration conditions. It is not known how long prey items remain attached to baleen of continuously feeding balaenids, but this likely involves seconds to minutes depending on prey density (Werth, 2001; Werth, 2012). Larger prey items of humpback whales and other lunge-feeding rorquals likely remain in contact with baleen for several seconds during the expulsive phase that precedes swallowing.

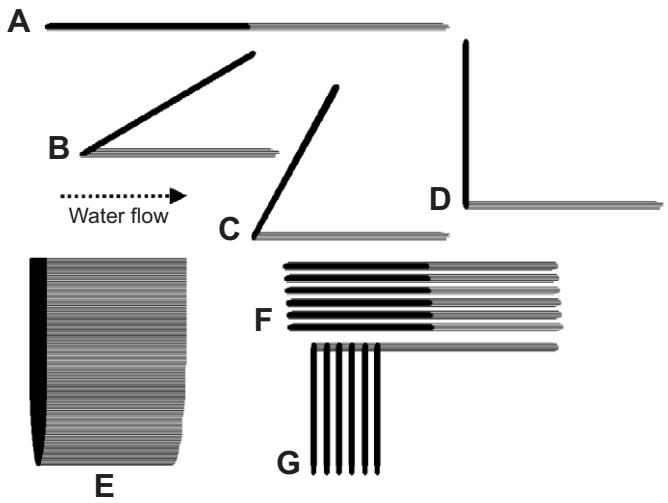

Fig. 2. Schematic diagram indicating positions of single and multiple baleen plates relative to water flow during flow tank testing. (A–D) Dorsal view of four positions of a single plate (A=0 deg, B=30 deg, C=60 deg, D=90 deg); in A, the medial edge of the plate with free fringes is to the left. No matter how plates are rotated relative to water flow, fringes always orient themselves downstream. (E) A single plate shown in lateral view. (F,G) An array of six plates shown in dorsal view, with all plates oriented at 0 deg (F) or 90 deg (G) to water flow; some tests also involved groups of multiple plates turned 30 or 60 deg to water flow, as in B and C.

Kinematic analysis

In the second series of experiments, the 'behavior' (spacing, movement and interaction) of fringes was recorded and analyzed. Kinematic sequences were videotaped from the viewing window and underwater from the testing chamber with a digital recording endoscope (VideoFlex SD, Umarex-Laserliner, Arnsberg, Germany) with an illuminated 17 mm camera head (5/25/50 cm focal distances) that recorded JPEG still images and AVI video (standard speed, 30 frames s^{-1}). The camera was fixed in position in the testing chamber or outside the viewing window so that it could record in ambient light or using built-in illumination. Most sequences were shot laterally, but some dorsal sequences were used as well, especially for multiple-plate testing (unless stated otherwise, data are from lateral views). Digital sequences (N=340) and images (N=378) were downloaded and analyzed on a Dell Optiplex 745 or Dimension D610 computer using Kinovea 0.8.15 video chronometer and motion analysis software (Boston, MA, USA). Each sequence lasted 20 s (total 68 min footage). Sequences were analyzed to detect movement of baleen fringes as well as capture of buoyant particles. Principal kinematic variables included: particle velocity and acceleration, movement and spacing of free fringes of baleen, and distance along a fringe from its origin on the baleen plate. All variables were tracked relative to observational references (fixed grid background or baleen plates), with playback at 10–100% of original speed or frame-by-frame, synchronized to time coding. The software allowed for magnification, plane perspective, tracking of path distance and velocity measurement, which was applied to suspended particles and/or baleen fringes in motion during flow tank testing.

To determine the extent to which baleen fringes moved due to incident water flow as well as contact from adjacent fringes, distances separating fringes (from the same or other plates), *d*, were measured and recorded. Individual fringes noted in kinematic sequences were counted in the analysis only when it was certain that the fringe locations were ≥1 cm from the plate, so as to exclude from this analysis the influence of immobile or less-mobile fringe sections where they emerged from the plate matrix. Kinematic sequences focused on individual fringes, and *d* between each fringe and other fringes (from the same or other plates, each fringe verified to be not less than 1 cm from its plate margin) was recorded as a measurement of inter-fringe distance (IFD). For each recorded sequence at least 30 fringes were analyzed for IFD measurement.

RESULTS

Comparative morphometrics

Baleen from bowhead and humpback whales differed in size (Fig. 1), which affected the number of total fringes. Plates also differed in triangular shape, which, along with varying fringe length (Table 1), affected the number of fringes that extended beyond the plate margin at any particular location. Measurements (Table 1) revealed major differences: bowhead baleen fringes were approximately twice as long with half the diameter of humpback fringes, and overall fringe density was three times as great in bowheads as in humpbacks. Two distinct fringe sizes (large and small, or outer and inner) have been described emanating from individual plates of some whales (Pivorunas, 1976), but no such discrepancy was observed here: all fringes of all plates of both tested species exhibited consistent measures of length, diameter and density (ANOVA, P=0.73).

Influence of flow velocity

In tests of particle capture *versus* incident *v*, multiple plate 'mini-racks' of both species captured more neutrally buoyant particles than did individual plates (Fig. 3). Overall, bowhead baleen proved far better at capture, except for single plates at higher *v* (≥75 cm s^{-1}). For multiple plate arrays, bowhead baleen samples invariably captured significantly (P=0.02) more particles than humpback baleen (Fig. 3). As *v* increased, more particles struck baleen fringes, as observed in videotaped sequences. However, these often did not remain on the fringes long enough (≥2 s) to qualify as captured, especially on the thin, highly mobile bowhead fringes. In fact, the high mobility of the bowhead fringes at higher *v* (≥75 cm s^{-1}) was correlated in kinematic sequences with particles being dislodged and swept away by other fringes. This was less apparent in tests with multiple plates, in which there were so many fringes that a dense mat was created. For single plates, the optimum *v* for particle capture was 30 cm s^{-1} with bowhead baleen and 75 cm s^{-1} with humpback baleen. For multiple plates, humpback baleen captured the most particles at the same *v* (75 cm s^{-1}), but in bowheads, multiple plates captured particles best at twice the *v* that was found to be best for single plates (60 *versus* 30 cm s^{-1}).

Trials conducted in different water temperatures yielded no difference in results, nor did the use of freshwater *versus* seawater in the flume affect filtration in these experiments.

Effects of fringe spacing and motion

To determine the mechanism directly responsible for the varying capture rates in the different whale species with Δ*v*, kinematic sequences recorded by the endoscopic camera were analyzed for data regarding fringe spacing, movement and interaction, using methodology described above. Fig. 4 shows the relationship between *v* and IFD in both species tested. For individual bowhead plates, the effect of *v* on IFD, and hence ϕ, was significant (P=0.04): at higher *v* (>50 cm s^{-1}), fringes showed substantial mobility and separation (hence increased IFD). This also proved true to a lesser extent with single humpback plates (Fig. 4). However, for multiple-plate arrays, IFD decreased markedly at all flow levels (with little effect from *v*). Although individual bowhead plates showed greater IFD, and thus higher ϕ, than individual humpback plates, multiple bowhead plates showed lower ϕ than multiple-plate arrays of humpback baleen (Fig. 4). IFD varies

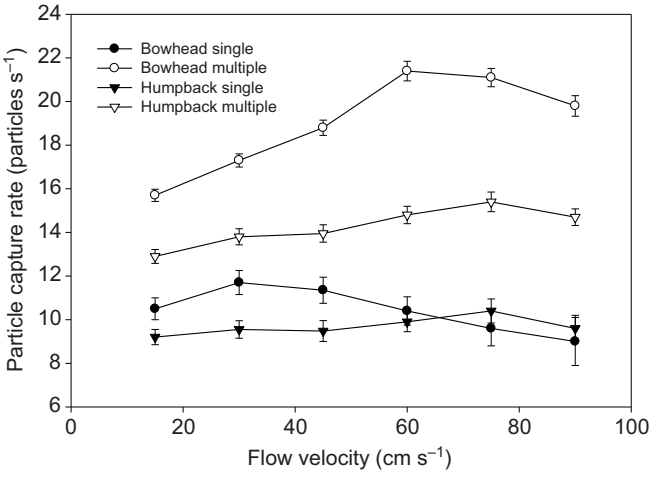

Fig. 3. In both bowhead and humpback whales, 'mini-racks' of multiple plates (parallel to flow, in position A from Fig. 2) captured more particles (defined here as particle contact with baleen fringe for ≥2 s, though capture rate shown is per newly caught particles per second) than did single plates. As water flow velocity increases, more particles strike fringes yet they are quickly dislodged, especially with bowhead baleen. Bowhead baleen captures more particles than humpback baleen, except for single plates at higher flow velocities.

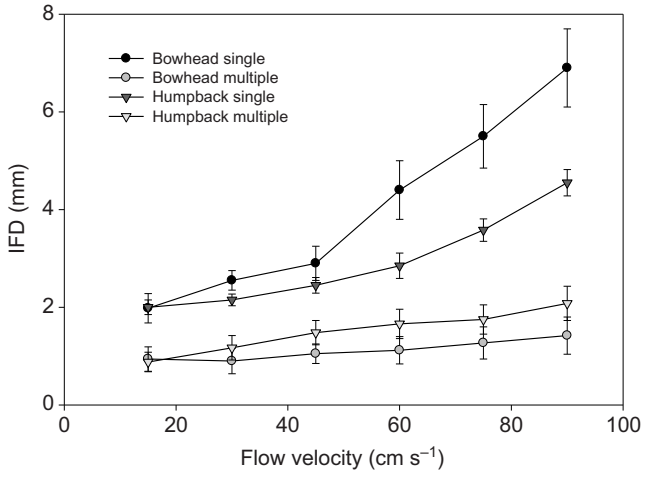

Fig. 4. Inter-fringe distance (IFD) *versus* water flow velocity. IFD was measured at points along fringes ≥1 cm from baleen plate (combined data from lateral and dorsal views). Note the increasing porosity (ϕ; as measured by IFD) as water flow velocity increases (with a greater range of ϕ at high flow velocity, especially in bowhead; error bars are ±1 s.d.), and the higher ϕ of finely fringed bowhead than coarse-fringed humpback baleen when tested with a single plate, but not with multiple plates, in which bowhead fringes from adjacent plates interact to lower ϕ.

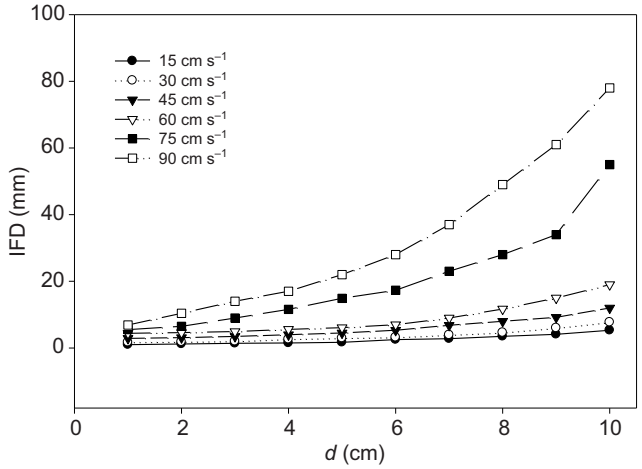

Fig. 5. Inter-fringe distance (IFD; mm) measured along free fringes of single plate of bowhead baleen at varying distance, *d*, from origin of fringe at emergence from the plate matrix. Note increased fringe separation (and increased ϕ) as *v* increases and as *d* increases (at all *v*).

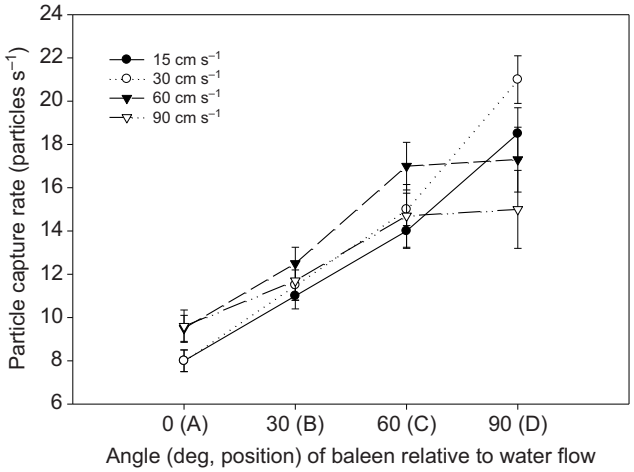

Fig. 7. Particles more easily strike fringes as baleen (here, 'mini-racks' of multiple plates, bowhead only) rotate perpendicular to water flow (increasing α), yet particles also more readily dislodge, especially at higher *v*.

considerably by fringe and over time, given that fringes undulate and waver in current flow. Nonetheless, as *d* (the distance along a fringe from the plate margin where it originates) increases, there are fewer entangling interactions with adjacent fringes, as revealed by kinematic analysis, and thus IFD increases with *d* (Fig. 5). This effect is even greater at higher *v*.

Influence of baleen position

Trials were conducted to test the influence of baleen position (attack angle α) on both IFD and particle capture. Fig. 6 shows that in bowheads, fringe distances (and thus ϕ) are lowest when plates are parallel to incident flow (position A of Fig. 2, α=0 deg), representing outward flow from the mouth's center to its sides. As α increases, IFD increases, for all *v*, but with a greater effect seen at higher *v* (Fig. 6). As noted above, IFD values vary greatly; it was difficult to measure IFD in multiple-plate trials. The effect of α on IFD is greatest with plates completely perpendicular to incident flow (α=90 deg). Similarly, capture also increased as α increased with plate rotation (in fact best seen with multiple plates; Fig. 7), though at high *v* (≥60 cm s^{-1}), capture levels off or slightly declines.

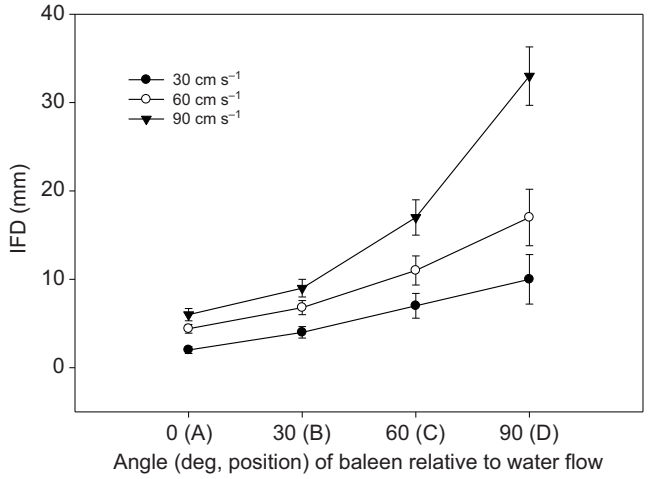

Fig. 6. At all *v*, ϕ [as measured by inter-fringe distance (IFD); data here from multiple bowhead plate testing] is lowest with plates parallel to flow, as α decreases. ϕ increases as turbulence is generated as α increases when plates are turned perpendicular to flow.

DISCUSSION

Comparative morphometrics

As all previous studies have reported, baleen of bowhead and right whales is long and finely fringed, whereas that of humpback and other balaenopterid whales is coarser, with shorter, thicker fringes. Measurements for this study (total *N*=290) confirm that differences (Table 1) are statistically significant (ANOVA, *P*=0.04). This has obvious consequences for feeding, and is an apparent adaptation. It is evident that balaenid baleen is specialized for preying chiefly upon tiny (~1 mm) copepods, and that of humpbacks for larger (5–20 cm) prey including schooling fish (e.g. sand lance, herring, capelin) and krill (Clapham and Mead, 1999). Although the distinctions between continuous skim feeding and intermittent lunge feeding are clear, there is ecological and morphological evidence that at least one rorqual, the sei whale (*Balaenoptera borealis*), also skim feeds (Brodie and Vikingsson, 2009). The pygmy right whale (*Caperea marginata*), the only member of Neobalaenidae, has unknown foraging habits and feeding mechanisms (Sekiguchi et al., 1992), and oral anatomy somewhat intermediate between rorquals and right whales (Kemper, 2009; Fordyce and Marx, 2013).

Although balaenid and balaenopterid plates differ in length, width and curvature, mysticete baleen plates are remarkably uniform in anteroposterior thickness (mean ± s.d. thickness=3.56±0.17 mm, *N*=64 plates of four species, including bowhead and humpback plus North Atlantic right and fin whales, *Eubalaena glacialis* and *Balaenoptera physalus*, respectively). Young's extensive morphometric analysis (Young, 2012) reports thickness and other baleen parameters from numerous mysticete species, including those (such as the gray whale, *Eschrichtius robustus*) that were notably absent from the project reported here.

The primary reason for measuring baleen fringe density and related parameters for this study was to determine how they might affect biomechanical properties, especially ϕ. In short, the principal basis for the differences in particle capture and fringe 'behavior' described here can be ascribed to differing length, diameter and density of bowhead *versus* humpback baleen. The wider fringes of

humpback baleen conceivably allow more particles to be struck and potentially captured, and single plates of humpback baleen proved better than bowhead baleen at capturing fast-flowing particles (Fig. 3), but in all other circumstances the longer, denser bowhead fringes captured more particles. The greater density of bowhead fringes, especially when multiple plates are combined to produce a more realistic simulation of an actual rack, enables baleen of this species to capture more particles under nearly all circumstances. Although in some instances the high rate of motion of the bowhead fringes dislodged and swept away particles that had made contact with other fringes, the advantage of these long, thin, highly mobile fringes is in undulating and interlocking to form a dense mat for better filtration. Mayo and colleagues concluded that ϕ of right whale baleen is equivalent to a 333 μm plankton net (Mayo et al., 2001).

Effects of flow velocity and fringe spacing

Kinematic analysis confirmed the functional difference between these species lies in the greater number and length of bowhead baleen fringes; at high v, these move apart, increasing IFD and opening gaps that raise ϕ, whereas as fringes from more and more plates interact, they continue to undulate in the current yet become entangled, forming a tightly woven mat (with lower IFD) that explains the greater capture seen in Fig. 3. As d increases, IFD likewise increases as a result of lessened interaction with adjacent fringes, especially at higher v (Fig. 5). The result is that bowhead fringes waver more, especially in high current flow (increased v), which would tend to increase rather than decrease ϕ, making baleen less likely to capture small particles. However, this is mitigated to a great extent by the sheer number of fringes on bowhead baleen, which, when combined with their notable length, increases their interaction, forming a dense mat that in fact decreases ϕ, making the baleen a more effective filter, especially for small particles such as the tiny copepods that bowheads primarily prey upon. Because humpback fringes are shorter, thicker (coarser) and fewer in number, they are substantially less mobile; they move and interact less, such that interactions between adjacent plates does decrease ϕ somewhat (Fig. 4), although this is far less dependent on v than it is with bowhead baleen. In sum, bowhead baleen plates become in some ways more porous at higher v (as revealed by increasing IFD), but fringe interactions ultimately have the effect of lowering ϕ, such that bowhead baleen becomes less porous as v increases. The difference is seen, dramatically, when single *versus* multiple baleen plates are tested together (Figs 3, 4). In the end, ϕ is clearly flow-dependent, particularly in finely fringed balaenid baleen.

Comparison of results from these laboratory experiments with data collected by field tagging of foraging whales indicates a close correspondence of measures of swimming speed, filtration flow and maximum particle capture. In both the bowhead and humpback baleen tested in these flow tank trials, the particle capture rate for multiple plates decreases at v>75 cm s^{-1}. This velocity corresponds perfectly with what has been measured as the filtration v in ram-foraging bowhead whales [75 cm s^{-1} (Simon et al., 2009)], and is very close to what has been estimated as the filtration v in foraging fin whales [80 cm s^{-1} (Goldbogen et al., 2007)]. This equivalence adds a valuable ecological context to these experimental results, and strongly suggests that the tagged whales were foraging at the optimal filtration rate for their baleen.

Influence of baleen position

As α increases, IFD increases, especially at higher v (Fig. 6), and this relates to particle capture (Fig. 7), which decreases in bowhead baleen at the highest v. With α=0 deg, fringes are held close together (hence low IFD) by strong, laminar current flow; as α rises to 90 deg, fringes splay and waver, though their distal portions often interact, especially with fringes from other plates. Kinematic analysis of the effect of plate orientation on both IFD and capture reveals that fringes are more mobile with higher flow, so that they often strike more particles, but that waving fringes more readily dislodge particles before they can be counted as captured (i.e. <2 s). As a result, ϕ is lowest with plates parallel to flow (representing flow outward from the center of the mouth), and ϕ increases as α rises (to the 90 deg position), apparently (based on IFD recorded from kinematic sequences) due to generation of turbulence. This has important consequences depending on the direction(s) of intraoral flow, which has been much speculated upon (Werth, 2004) but has not been reliably documented, and which may involve cross-flow or other tangential filtration, in contrast to the orthodox view of the mysticete filtration apparatus acting as a dead-end, flow-through sieve (Werth, 2011).

There was, in addition to the horizontal (anteroposterior and mediolateral) flow described here, a vertical gradient to the oral flow recorded in these experiments. This is noteworthy given the highest fringe density, and hence the lowest ϕ is at the plate's ventral terminus, where the most particles (~70%) were observed to be captured. The extent to which any element of vertical as well as horizontal flow occurs in whale mouths is unknown (and the subject of ongoing investigation), but the complexities of three-dimensional flow associated with mysticete oral filtration are likely to be substantial. In bowhead and right whales, this may depend on whether a whale is skimming at the sea surface or underwater. In bowheads it may also depend on the distance from the anterior oral opening, where prey-laden water enters at the subrostral gap, and to the posterior oral opening, where filtered water exits the mouth behind the lips.

Baleen biomechanics

Although findings here relate to biomechanical properties such as bending stiffness and Young's modulus, basic laboratory materials testing of these and other properties of elasticity and tensile and compressive strength, for example, is sorely lacking and an obvious avenue of future baleen research. Nonetheless, data provided here on ϕ and α are essential to a thorough, realistic understanding of the function of baleen plates and fringes in dynamic circumstances of filter feeding, which involve high forces and flows, including potential Bernoulli and Venturi effects (Werth, 2004). From this study it is clear that although bowhead and humpback baleen plates are of similar thickness – and the flow tank tests used specimens of identical size – both the longer, narrower fringes of bowheads and their similarly longer, narrower plates confer different functional capacities. The shorter, coarser fringes of humpbacks are less mobile, so that ϕ in this species (and presumably in other rorquals) is less flow-dependent than in balaenid whales, which exhibit a greater degree of ϕ that depends greatly on flow parameters.

Consider that mysticete filtration currents vary from a gradual, steady stream in continuously skim-feeding balaenids to powerful and sudden (near-explosive) expulsion events in lunge-feeding rorquals and benthic suction-feeding gray whales. The differences in fluid friction and hydrostatic pressure embodied by these markedly disparate phenomena must be vast. Although actual values have not been obtained, it can be estimated (author's calculations) that baleen is routinely subjected to pressures ranging from 0.2 to 400 kPa, with peak pressures potentially reaching 800–1000 kPa or more, with the equivalence of 10^6 N m^{-2} of force. To withstand such dynamic forces, baleen must be a remarkably strong yet pliant material. No fringes broke in these experiments, and all returned to their original

positions despite pronounced bending, showing hysteresis loops of perfect elasticity when loaded and unloaded from water flow.

As noted previously, all baleen specimens were kept submerged in flowing water for at least 7 days prior to flow tank testing. However, limited initial trials (data not shown) used baleen that had been dried and maintained in air for long periods of time, in some cases for months since post mortem collection. Air-dried baleen yielded substantially different results than baleen treated by water soaking in both indicators of ϕ (particle capture and IFD), although the differences were not statistically significant. Relative to baleen treated in water, dried baleen captured fewer particles (at all v tested; t-test, P=0.24) and displayed greater IFD measurements (again, at all v; t-test, P=0.19). These results, along with subjective observations, suggest that baleen fringes that had been dried in air were stiffer and had lost much of their flexibility, although none failed during loading.

Future research

Baleen is dynamic not only in function but also as a growing tissue. The relationship between baleen growth and the biomechanics of feeding (by age, species, etc.) demands investigation. The particles used in these experiments are non-adhesive, non-elusive and much smaller than typical prey. Ongoing flow tank experiments (Werth, 2012) explore capture of copepods and other known prey. The extent to which baleen can become fouled by oil and other contaminants of varying refinement and viscosity is another avenue of future research. This topic has been preliminarily explored (Geraci and St Aubin, 1982; Geraci, 1990), but controlled flow tank experiments are ideally suited to address this crucial issue in greater detail.

A vexing question concerning the functional morphology of mysticetes is how they clean their oral filters or prevent it from clogging (Werth, 2001). This is more of an issue for balaenids because of their finely fringed baleen and tiny prey, and less so for rorquals and gray whales, which are intermittent suspension feeders that trap larger prey with coarser baleen. Several hypotheses have been advanced (Werth, 2001) to address means by which mysticetes could clean their oral filters. However, results of these flow tank experiments, especially the findings concerning baleen position and α relative to flow, together with improved understanding of intraoral balaenid water flow, suggests that use of cross-flow filtration largely precludes clogging of the filter, which acts unlike a traditional throughput filter or sieve and more like filters used in industry and, critically, in other aquatic vertebrates (Sanderson et al., 2001). Given that filter-feeding fishes and balaenid and rorqual whales all operate at similarly moderate Reynolds numbers and fairly low filtration velocities (Sanderson et al., 2001; Goldbogen et al., 2007; Simon et al., 2009), it might be expected that they share the same underlying filtration mechanisms. Clearly this presumption requires further investigation, both from further flow tank testing and computational fluid dynamics, for which work is ongoing (Werth, 2011), and ideally from *in vivo* biologging data regarding intraoral water flow and baleen function.

The extent to which flow-induced drag is generated around and within baleen racks and the subsequent role this plays in mysticete feeding are poorly understood, presenting obvious additional avenues for future research. Bernoulli and Venturi effects and related forces that promote or restrict flow may be important in both continuous (Werth, 2004) and intermittent filtration (Potvin et al., 2009) of mysticetes. In lunge-feeding rorquals, flow-induced pressures may play a crucial role in inflating the buccal cavity (Potvin et al., 2009), causing a pressure drop in the mouth and thus influencing filtration. It is likely that the smaller pore sizes (decreased ϕ) within a baleen rack that are generated during filtration (especially at high v) serve to increase drag, in turn further reducing ϕ in a spiraling loop of positive feedback. This would greatly constrain the foraging speeds of all baleen whales, and may explain the close agreement between this study's optimal flow v for particle capture (~75 cm s^{-1}) and documented foraging speeds of balaenid and balaenopterid whales (Goldbogen et al., 2007; Simon et al., 2009). In sum, results of these flow tank experiments strongly suggest that baleen's porosity and related biomechanical properties create functional constraints or ecological limits on mysticete feeding. This complex topic would be best addressed by a combination of controlled experiments, computer simulations and field tagging studies.

In the continued absence of *in vivo* intraoral data – hopefully to be remedied by placement of digital tags within the mouth (e.g. on the baleen, palate or lips) or by obtaining data from telemetric devices that are swallowed – our best approximation of intraoral forces and flows comes from functional morphology investigations of mysticete tissues tested under conditions presumed to be as realistic as possible, and integration of such studies with field data. Given that *ex vivo* tissue studies of baleen have not previously been attempted, the study presented here advances considerably our meager understanding of mysticete functional morphology and biomechanics.

LIST OF SYMBOLS AND ABBREVIATIONS

d	distance
IFD	inter-fringe distance
v	flow velocity
α	angle of attack (of baleen plates)
ϕ	porosity

ACKNOWLEDGEMENTS

Samples of bowhead baleen are from animals harvested by Inupiat hunters of the Alaska Eskimo Whaling Commission in accordance with their special exemption to the US Marine Mammal Protection Act and other national and international restrictions. I am grateful to these hunters for allowing me to examine and sample their whales. Bowhead tissues were collected under permit no. 519 issued to T. F. Albert of the North Slope Borough (Alaska) Department of Wildlife Management by the National Marine Fisheries Service. Samples of humpback baleen are from stranded animals collected by the New England Aquarium under NMFS permit no. 932-1489. I am indebted to I. Robertson for construction of the flow tank and S. Vogel for advice on its design, and to students for assistance with data collection and logistics. I thank S. L. Sanderson for valuable discussion regarding experimental design and methodology, and H. Ito, J. Goldbogen, N. Pyenson, M. Simon, P. Madsen, F. Fish, J. Reidenberg, J. van der Hoop, B. Kot, C. Marshall, S. Pinto, T. Ford, R. Payne, S. Kraus, J. C. George, T. Sformo, R. Suydam, D. Wiley, C. Mayo, M. Baumgartner and anonymous reviewers for information, ideas and feedback regarding whale feeding and this study in particular.

FUNDING

Funding was provided by faculty fellowship grants from Hampden-Sydney College, and by Mednick and Harris Awards from the Virginia Foundation for Independent Colleges.

REFERENCES

Braithwaite, L. F. (1983). *Final Report: Effects of Oil on The Feeding Mechanism of The Bowhead Whale, Project RU 679 (Baleen Plate Fouling)*. Prepared for the US Department of the Interior under contract no. AA851-CTO-55. Brigham Young University, Provo, UT, USA.

Brodie, P. and Vikingsson, G. (2009). On the feeding mechanisms of the sei whale (*Balaenoptera borealis*). *J. Northw. Atl. Fish. Sci.* **42**, 49-54.

Carroll, G. M., George, J. C., Lowry, L. F. and Coyle, K. O. (1987). Bowhead whale (*Balaena mysticetus*) feeding near Point Barrow, Alaska, during the 1985 spring migrations. *Arctic* **40**, 105-110.

Clapham, P. J. and Mead, J. G. (1999). *Megaptera novaeangliae*. *Mammalian Species* **604**, 1-9.

Fordyce, R. E. and Marx, F. G. (2013). The pygmy right whale *Caperea marginata*: the last of the cetotheres. *Proc. R. Soc. B* **280**, 20122645. doi:10.1098/rspb.2012.2645

Friedlaender, A. S., Hazen, E. L., Nowacek, D. P., Halpin, P. N., Ware, C., Weinrich, M. T., Hurst, T. and Wiley, D. (2009). Diel changes in humpback whale *Megaptera novaeangliae* feeding behavior in response to sand lance *Ammodytes* spp. behavior and distribution. *Mar. Ecol. Prog. Ser.* **395**, 91-100.

Fudge, D. S., Szewciw, L. J. and Schwalb, A. N. (2009). Morphology and development of blue whale baleen: an annotated translation of Tycho Tullberg's classic 1883 paper. *Aquatic Mammals* **35**, 226-252.
Geraci, J. R. (1990). Physiological and toxic effects on cetaceans. In *Sea Mammals and Oil: Confronting the Risks* (ed. J. R. Geraci and D. St. Aubin), pp. 167-197. New York: Academic Press.
Geraci, J. R. and St Aubin, D. J. (1982). *Final Report: Studies of the Effects of Oil on Cetaceans*. Prepared for the US Department of the Interior under contract no. AA551-CT9-29. University of Guelph, ON, Canada.
Goldbogen, J. A., Calambokidis, J., Shadwick, R. E., Oleson, E. M., McDonald, M. A. and Hildebrand, J. A. (2006). Kinematics of foraging dives and lunge-feeding in fin whales. *J. Exp. Biol.* **209**, 1231-1244.
Goldbogen, J. A., Pyenson, N. D. and Shadwick, R. E. (2007). Big gulps require high drag for fin whales lunge feeding. *Mar. Ecol. Prog. Ser.* **349**, 289-301.
Goldbogen, J. A., Calambokidis, J., Croll, D. A., Harvey, J. T., Newton, K. M., Oleson, E. M., Schorr, G. and Shadwick, R. E. (2008). Foraging behavior of humpback whales: kinematic and respiratory patterns suggest a high cost for a lunge. *J. Exp. Biol.* **211**, 3712-3719.
Goldbogen, J. A., Calambokidis, J., Oleson, E., Potvin, J., Pyenson, N. D., Schorr, G. and Shadwick, R. E. (2011). Mechanics, hydrodynamics and energetics of blue whale lunge feeding: efficiency dependence on krill density. *J. Exp. Biol.* **214**, 131-146.
Goldbogen, J. A., Calambokidis, J., Kroll, D. A., McKenna, M. F., Oleson, E., Potvin, J., Pyenson, N. D., Schorr, G., Shadwick, R. E. and Tershy, B. (2012). Scaling lunge feeding performance in rorqual whales: mass-specific energy expenditure increases with body size and progressively limits diving capacity. *Funct. Ecol.* **26**, 216-226.
Kemper, C. M. (2009). Pygmy right whale *Caperea marginata*. In *Encyclopedia of Marine Mammals*, 2nd edn (ed. W. F. Perrin, B. Würsig and J. G. M. Thewissen), pp. 939-941. San Diego, CA: Academic Press.
Kot, B. W. (2005). Rorqual whale surface-feeding strategies: biomechanical aspects of feeding anatomy and exploitation of prey aggregations along tidal fronts. MSc thesis, University of California, Los Angeles, CA, USA.
Kot, B. W. (2009). Rorqual whale (Balaenopteridae) lunge-feeding behaviors, processes and mechanisms. PhD thesis, University of California, Los Angeles, CA, USA.
Lambertsen, R. (1983). Internal mechanism of rorqual feeding. *J. Mammal.* **64**, 76-88.
Lambertsen, R. H., Rasmussen, K. J., Lancaster, W. C. and Hintz, R. J. (1989). *Final Report: Functional Morphology of The Mouth of The Bowhead Whale and its Implications For Conservation*. Prepared for the North Slope Borough, AK, under contract no. 87-113. Ecosystems Inc., Philadelphia, PA, USA.
Lambertsen, R. H., Rasmussen, K. J., Lancaster, W. C. and Hintz, R. J. (2005). Functional morphology of the mouth of the bowhead whale and its implications for conservation. *J. Mammal.* **86**, 342-352.
Lowry, L. F. (1993). Foods and feeding ecology. In *The Bowhead Whale* (ed. J. J. Burns, J. J. Montague and C. J. Cowles), pp. 201-238. Lawrence, KS: Society for Marine Mammalogy.
Mayo, C. A., Letcher, B. H. and Scott, S. (2001). Zooplankton filtering efficiency of the baleen of a North Atlantic right whale, *Eubalaena glacialis*. *J. Cetacean Res. Manag.* **2**, 225-229.
Nowacek, D. P., Johnson, M. P., Tyack, P. L., Shorter, K. A., McLellan, W. A. and Pabst, D. A. (2001). Buoyant balaenids: the ups and downs of buoyancy in right whales. *Proc. Biol. Sci.* **268**, 1811-1816.
Nowacek, D. P., Friedlaender, A. S., Halpin, P. N., Hazen, E. L., Johnston, D. W., Read, A. J., Espinasse, B., Zhou, M. and Zhu, Y. (2011). Super-aggregations of krill and humpback whales in Wilhelmina Bay, Antarctic Peninsula. *PLoS ONE* **6**, e19173.
Orton, L. and Brodie, P. (1987). Engulfing mechanics of fin whales. *Can. J. Zool.* **65**, 2898-2907.
Pfeiffer, C. (1992). Cellular structure of terminal baleen in various mysticete species. *Aquatic Mammals.* **18**, 67-73.
Pinto, S. J. D. (2011). On the filtration mechanisms and oral anatomy of lunge-feeding baleen whales. MSc thesis, University of British Columbia, BC, Canada.
Pivorunas, A. (1976). A mathematical consideration of the function of baleen plates and their fringes. *Sci. Rep. Whales Res. Inst.* **28**, 37-55.
Pivorunas, A. (1977). The fibrocartilage skeleton and related structures of the ventral pouch of balaenopterid whales. *J. Morphol.* **151**, 299-313.
Pivorunas, A. (1979). The feeding mechanisms of baleen whales. *Am. Sci.* **67**, 432-440.
Potvin, J., Goldbogen, J. A. and Shadwick, R. E. (2009). Passive versus active engulfment: verdict from trajectory simulations of lunge-feeding fin whales *Balaenoptera physalus*. *J. R. Soc. Interface* **6**, 1005-1025.
Potvin, J., Goldbogen, J. A. and Shadwick, R. E. (2010). Scaling of lunge feeding in rorqual whales: an integrated model of engulfment duration. *J. Theor. Biol.* **267**, 437-453.
Pyenson, N. D., Goldbogen, J. A., Vogl, A. W., Szathmary, G., Drake, R. L. and Shadwick, R. E. (2012). Discovery of a sensory organ that coordinates lunge feeding in rorqual whales. *Nature* **485**, 498-501.
Reeves, R. R. and Leatherwood, S. (1985). *Bowhead Whale*, *Balaena Mysticetus,* Linnaeus 1758. In *Handbook of Marine Mammals. Vol. 3: The Sirenians and Baleen Whales* (ed. S. H. Ridgway and R. Harrison), pp. 305-344. San Diego, CA: Academic Press.
Sanderson, S. L., Cheer, A. Y., Goodrich, J. S., Graziano, J. D. and Callan, W. T. (2001). Crossflow filtration in suspension-feeding fishes. *Nature* **412**, 439-441.
Sekiguchi, K., Best, P. B. and Kaczmaruk, B. Z. (1992). New information on the feeding habits and baleen morphology of the pygmy right whale *Caperea marginata*. *Mar. Mamm. Sci.* **8**, 288-293.
Simon, M. J., Johnson, M., Tyack, P. and Madsen, P. T. (2009). Behaviour and kinematics of continuous ram filtration in bowhead whales (*Balaena mysticetus*). *Proc Biol. Sci.* **276**, 3819-3828.
St Aubin, D. J., Stinson, R. H. and Geraci, J. R. (1984). Aspects of the structure and composition of baleen, and some effects of exposure to petroleum hydrocarbons. *Can. J. Zool.* **62**, 193-198.
Szewciw, L. J., de Kerckhove, D. G., Grime, G. W. and Fudge, D. S. (2010). Calcification provides mechanical reinforcement to whale baleen α-keratin. *Proc. Biol. Sci.* **277**, 2597-2605.
Tullberg, T. (1883). The structure and development of blue whale baleen. *Nova Acta Regiae Societatis Scientiarum Upsalensis* **3**, 1-36.
Vogel, S. (1996). *Life in Moving Fluids: The Physical Biology of Flow*, 2nd edn. Princeton, NJ: Princeton University Press.
Ware, C., Friedlaender, A. S. and Nowacek, D. P. (2011). Shallow and deep lunge feeding of humpback whales in fjords of the West Antarctic Peninsula. *Mar. Mamm. Sci.* **27**, 587-605.
Werth, A. J. (2000). Marine mammals. In *Feeding: Form, Function and Evolution in Tetrapod Vertebrates* (ed. K. Schwenk), pp. 475-514. New York: Academic Press.
Werth, A. J. (2001). How do mysticetes remove prey trapped in baleen? *Bull. Mus. Comp. Zool.* **156**, 189-203.
Werth, A. J. (2004). Models of hydrodynamic flow in the bowhead whale filter feeding apparatus. *J. Exp. Biol.* **207**, 3569-3580.
Werth, A. J. (2011). *Cross-Flow Filtration in Baleen; or, Why Much of What You Think You Know About Mysticete Filter Feeding is Wrong* (Abstract). Proceedings of the 19th Biennial Conference of the Society for Marine Mammalogy, Tampa, FL, USA.
Werth, A. J. (2012). Hydrodynamic and sensory factors governing response of copepods to simulated predation by baleen whales. *Int. J. Ecol.* doi:10.1155/2012/208913.
Williamson, G. R. (1973). Counting and measuring baleen and ventral grooves of whales. *Scientific Reports of the Whales Research Institute* **25**, 279-292.
Young, S. (2012). The comparative anatomy of baleen: evolutionary and ecological implications. MSc thesis, San Diego State University, San Diego, CA, USA.